PHYSICAL REVIEW B VOLUME 26, NUMBER 9 1 NOVEMBER 1982

# Resistivity of spin-glasses

I. A. Campbell
*Physique des Solides, Université de Paris-Sud, 91405 Orsay, France*

P. J. Ford
*Physics Department, University of Witwatersrand, Johannesburg 2001, South Africa*

A. Hamzić
*Institute of Physics of the University and Faculty of Science, 41001 Zagreb, Yugoslavia*
(Received 2 April 1982)

We analyze experimental data on the temperature-dependent part of the resistivity of *Au*Fe, *Cu*Mn, *Ag*Mn, *Au*Mn, and *Au*Cr spin-glass alloys, using a model derived from the excitation approach of Walker and Walstedt. The model gives a satisfactory description of the experimental behavior for all the alloys. We find an energy scaling parameter for the excitation density of states that turns out to be approximately proportional to the spin-glass freezing temperature $T_g$. From the resistivity results we can estimate the local spin-relaxation time.

Most of the fundamental properties of spin-glasses remain incompletely understood, despite an intensive theoretical and experimental effort over the last few years. Among these basic properties are the magnetic excitation spectrum and the form of the excitations. The electrical resistivity is a potential source of information, and a number of models have been proposed that relate the resistivity to the magnetic excitations.[1] Walker and Walstedt[2] carried out a numerical calculation to estimate the excitation density of states for a spin-glass, starting with a Heisenberg Hamiltonian in which dilute magnetic spins are coupled through Ruderman-Kittel-Kasuya-Yosida (RKKY) interactions. We have found[3] that if we make certain assumptions we can get a satisfactory explanation for the temperature dependence of the resistivity of a spin-glass using the Walker-Walstedt excitation spectrum; we also find that the resistivity and the low-temperature magnetic specific heat are related.

Here we will show that for the canonical noble-metal–based spin-glass systems (*Cu*Mn, *Ag*Mn, *Au*Fe, *Au*Mn, and *Au*Cr) the available resistivity and specific-heat data can be analyzed coherently with the use of this approach. This indicates that the Walker-Walstedt spectrum is a reasonable approximation to the real spectrum in these systems. We find that the spin-glass freezing temperature $T_g$ is simply related to the energy scale of the excitation spectrum in each alloy. We also show that we can use the resistivity data to estimate the local-moment relaxation rate.

## EXPERIMENTAL DATA

Extensive systematic resistivity data have been obtained on these alloys by Mydosh *et al.*[4] and by Ford and Mydosh.[5] Following these authors, we will discuss the temperature-dependent part of the impurity resistivity defined by

$$\Delta\rho(T)=\rho(T)-[\rho(0)+\rho_i(T)]\ , \tag{1}$$

where $\rho(T)$ is the measured alloy resistivity, $\rho(0)$ is the residual resistivity, and $\rho_i(T)$ is the pure host resistivity. References 4 and 5 discuss the problems which can complicate this separation, in particular deviations from Matthiessen's rule in the phonon term. In addition, it is always necessary to extrapolate to estimate $\rho(0)$ and this can introduce considerable uncertainty in the low-temperature range of $\Delta\rho(T)$.

We have used tabulated data for $\Delta\rho(T)$ corresponding to the results reported in Refs. 4 and 5. Parts of these data were kindly put at our disposal by Professor J. A. Mydosh. For the magnetic specific heat we have used a variety of published data.[6–16]

## ANALYSIS

As discussed in Ref. 3, if we assume that the conduction-electron–excitation-interaction

strength is independent of energy, we can derive a phenomenological expression for the temperature-dependent scattering term in the spin-glass resistivity,

$$\Delta\rho(T)\alpha\int\frac{\Delta P(\Delta)/kT}{e^{\Delta/kT}-1}d\Delta\ . \tag{2}$$

Here $\Delta$ is the excitation energy and $P(\Delta)$ is the excitation density of states. For a given $P(\Delta)$, we can write

$$\Delta\rho(T)=\rho_\infty f(T/T^*)\ , \tag{3}$$

where the function $f$ is defined by the preceding equation and is normalized to saturation at $f(\infty)=1$. $\rho_\infty$ is the saturation value of $\Delta\rho(T)$ at high temperature and $T^*$ is an energy scaling parameter which we can define for a given $P(\Delta)$. We will discuss elsewhere the significance of the assumptions we have made to obtain Eq. (2).

We have chosen for the numerical calculations to use the histogram $P(\Delta)$ given by Walker and Walstedt (Ref. 2, Fig. 9). The low-energy end is illustrated in Fig. 1, where we define $kT^*$ as the energy interval shown. To see what effect a change in $P(\Delta)$ for small $\Delta$ would have, we have also calculated with a histogram inspired by Ref. 17, where it was suggested that $P(\Delta)$ should vary as $\Delta^2$ for small $\Delta$. In fact this changed the form of $f(T/T^*)$ rather slightly except for the region $T<0.1T^*$.

In the same model, we also derived a relationship between the low-temperature magnetic specific heat and the resistivity,[3]

$$C(T)=R\frac{d}{dT}\left[\frac{T\Delta\rho(T)}{\rho_\infty}\right]\ . \tag{4}$$

In this relationship the distribution $P(\Delta)$ does not enter explicitly and the only parameter which we need to know to relate the two independent low-

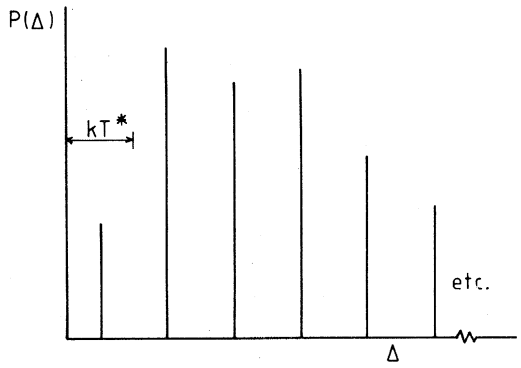


FIG. 1. Assumed excitation density of states $P(\Delta)$ as a function of energy $\Delta$ (following Ref. 2). $kT^*$ is defined as the energy scaling parameter.

temperature measurements is $\rho_\infty$. Now in principle we should know $\rho_\infty$ from the high-temperature limiting resistivity. In practice this is not so; at high temperatures where the interactions between the magnetic sites become relatively unimportant, Kondo resistivity behavior sets in; this is of course not allowed for in Eq. (2). The passage from interaction-dominated behavior to Kondo-dominated behavior has been discussed theoretically[18–20]; phenomenologically we find that from low temperatures up to about the spin-glass freezing temperature $T_g$ the form of the $\Delta\rho(T)$ curve is given quite accurately by our calculated $f(T/T^*)$; above $T_g$ there are deviations and at high temperatures the calculated curve saturates while the experimental curve drops as $T$ rises and always lies below the calculated curve. We ascribe this difference to the Kondo term, and we can estimate *a priori* the strength of the effect which we would expect in these concentrated alloys from Kondo-effect data at low concentrations, assuming that at high temperature the Kondo resistivity scales as the concentration. As we will see, we can get a reasonable estimate of $\Delta\rho(T)$ over the entire temperature range. We then proceed to analyze the experimental data as follows.

(i) If for a particular alloy both low-temperature specific heat and $\Delta\rho(T)$ data are available, we estimate $\rho_\infty$ by comparing the two sets of data using Eq. (4). With this $\rho_\infty$, we find the value of $T^*$ which gives the best fit to $\Delta\rho(T)$ up to about $T_g$. We then compare the calculated $\Delta\rho(T)$ curve with the experimental curve over the whole temperature range.

(ii) If only $\Delta\rho(T)$ data are available, a log-log plot of $\Delta\rho(T)$ against $T$ is compared with a log-log plot of $f(T/T^*)$, again for the temperature range below $T_g$. From the fit we can estimate both $\rho_\infty$ and $T^*$. This is a less satisfactory procedure and it would be of interest to have more specific-heat data particularly for *Au*Mn and *Au*Cr alloys. We will present the analysis of the various alloy systems before discussing the significance of the results.

## ANALYSIS OF ALLOY SYSTEMS

### *Au*Fe

Here we have available resistivity data from 4.2 to 300 K on 1- and 2-at. % alloys, and data on a 0.9-at % alloy from 0.5 to 40 K. Low-temperature specific heats have been reported at various concentrations.[6–8]

In Fig. 2, we give points for directly measured

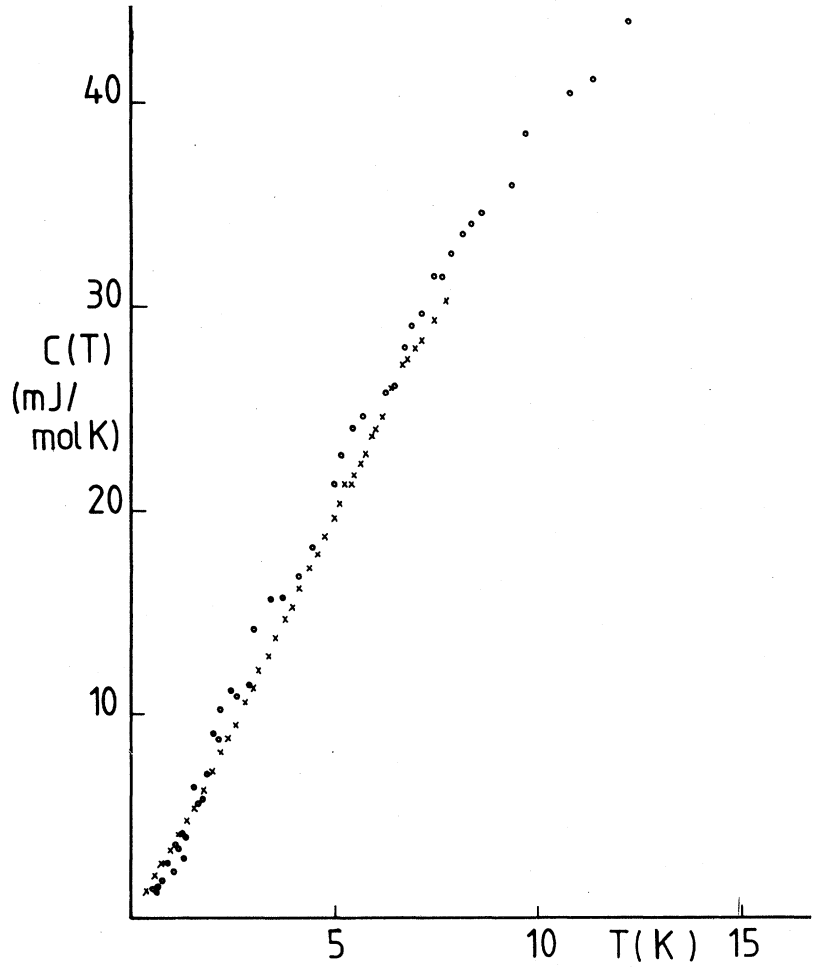


FIG. 2. Magnetic specific heat of *Au*Fe 0.9-at. % *Au*Fe. × denotes the direct measurement, Refs. 6 and 7. ○ is calculated from $\Delta\rho(T)$ data with Eq. (4) assuming $\rho_\infty = 0.5\ \mu\Omega$ cm.

magnetic specific heat for *Au*Fe alloys near 0.9-at. % Fe (Refs. 6 and 7) and points for

$$Rd/dT[T\Delta\rho(T)]/\rho_\infty$$

on an alloy of the same concentration, where we have chosen to put $\rho_\infty = 0.5\ \mu\Omega$ cm. The two curves are practically indistinguishable. We then plot, in Fig. 3, the experimental $\Delta\rho(T)$ on this same alloy together with the calculated curve using $\rho_\infty = 0.5\ \mu\Omega$ cm and $T^* = 4.0$ K. Finally in Fig. 4 for a 1-at. % sample we give the calculated and experimental $\Delta\rho(T)$ curves over the whole temperature range up to 300 K. The results are typical of the other concentrations. $\rho_\infty$ and $T^*$ values deduced from the analysis are given in Table I and Figs. 14 and 15.

### *Cu*Mn

The same type of comparison between specific-heat and resistivity data is given in Fig. 5 for three *Cu*Mn concentrations (specific heats estimated from measurements in Refs. 9–15). We deduce the fitting parameters $\rho_\infty$ and $T^*$ given in Table I. In Figs. 6 and 7 we show calculated and experimental $\Delta\rho(T)$ curves for *Cu*Mn 2.5 at % over two temperature ranges. It can be seen that at high temperature there is a considerable gap between the two curves. We can compare with Kondo-behavior data on much more dilute *Cu*Mn alloys, assuming that at high temperature the Kondo-resistivity term is proportional to the impurity concentration. From results on a 200-ppm alloy[21] we can estimate

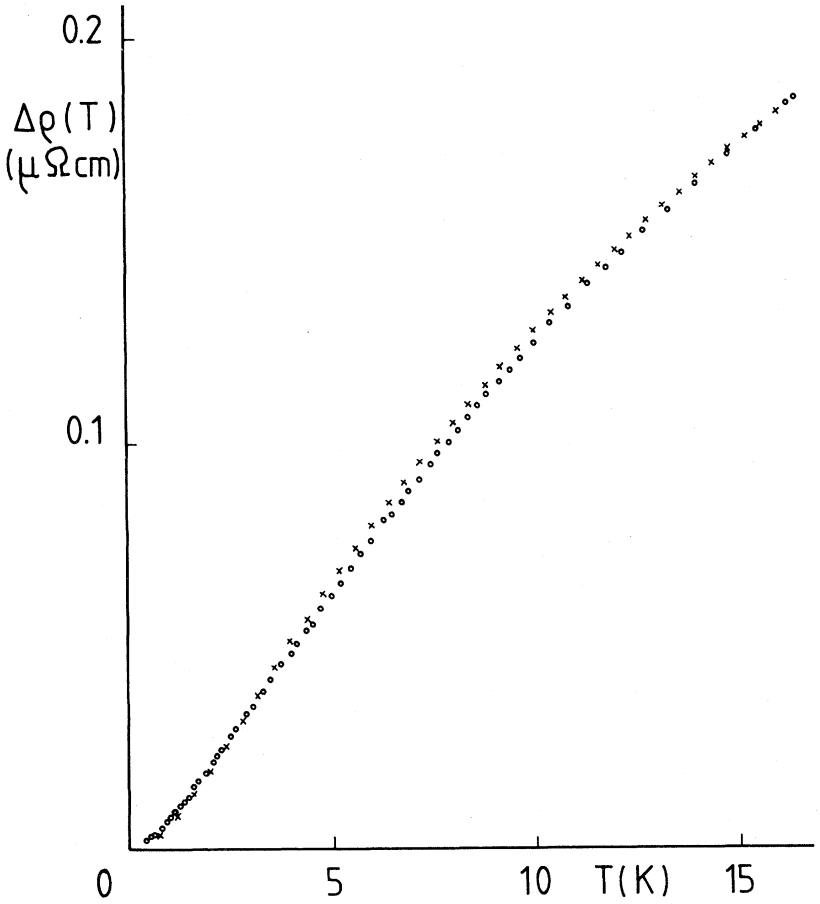


FIG. 3. Resistivity $\Delta\rho(T)$ as a function of temperature for 0.9-at. % *Au*Fe. ○ denotes experimental and × calculated data $\rho_\infty = 0.5\ \mu\Omega$ cm and $T^* = 4.0$ K.

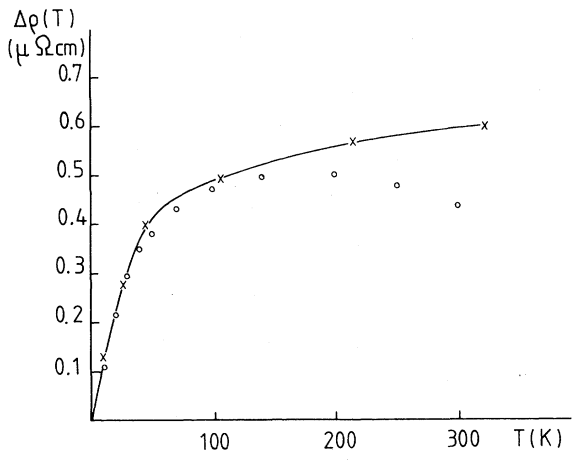


FIG. 4. Resistivity $\Delta\rho(T)$ for *Au*Fe 1 at. %*Au*Fe. ○ denotes experimental and × calculated data; $\rho_\infty = 0.7\ \mu\Omega$ cm and $T^* = 6$ K.

that for a 2.5-at. % alloy the Kondo-effect drop in resistivity from 20 K (i.e., $T \simeq T_g$) to 300 K would be about 1.6 $\mu\Omega$ cm. This is very close to the difference at 300 K between the experimental curve and the model curve calculated with the low-temperature fitting parameters, Fig. 7. Even though extrapolation of the Kondo term over such a wide concentration range is probably not very realistic, we can conclude that in the region above $T_g$ to a first approximation the spin-glass resistivity term and the Kondo term add to give the total $\Delta\rho(T)$, and that the $\rho_\infty$ estimated from the low-temperature data alone is compatible with the high-temperature behavior if allowance is made for the Kondo effect.

We have no Kondo-resistivity data comparable to that of Teixiera[21] for *Au*Fe, but results on low-concentration alloys over a narrower temperature range[22] suggest a weaker Kondo term than in *Cu*Mn.

TABLE I. Fitting parameters $\rho_\infty, T^*$ estimated as described in the text. $T_g$ is the cusp temperature on the same alloy.

| Alloy | $c$ at % | $\rho_\infty$ ($\mu\Omega$ cm) | $T^*$ (K) | $T_g$ (K) (Refs. 4 and 5) |
|---|---|---|---|---|
| *Au*Fe | 0.9 | 0.5 | 4.0 | 8 |
| | 1.0 | 0.65 | 6.0 | 8.5 |
| | 2.0 | 1.0 | 7.5 | 14 |
| *Cu*Mn | 1.0 | 1.0 | 4.0 | 11 |
| | 2.5 | 2.1 | 6.8 | 18 |
| | 4.4 | 3.5 | 11.0 | 27 |
| | 9.7 | 5.9 | 21.5 | 44 |
| *Ag*Mn | 1.1 | 0.35 | 1.1 | 5.5 |
| | 3.0 | 1.1 | 4.0 | 12 |
| | 5.4 | 1.55 | 5.1 | 19 |
| | 9.7 | 3.4 | 10.7 | 30 |
| *Au*Cr | 0.9 | 0.8 | 4.5 | 14 |
| | 3.3 | 3.1 | 12.0 | 35 |
| | 4.9 | 4.5 | 16.5 | 50 |
| | 7.9 | 6.8 | 23 | 78 |
| | 10.6 | 9.0 | 30 | 100 |
| *Au*Mn | 1.5 | 0.5 | 2.0 | 7.0 |
| | 2.8 | 0.7 | 2.6 | 11 |
| | 4.6 | 1.5 | 6.1 | 16.5 |
| | 7.7 | 3.2 | 11.2 | 25 |
| | 11.8 | 6.2 | 20 | 34 |

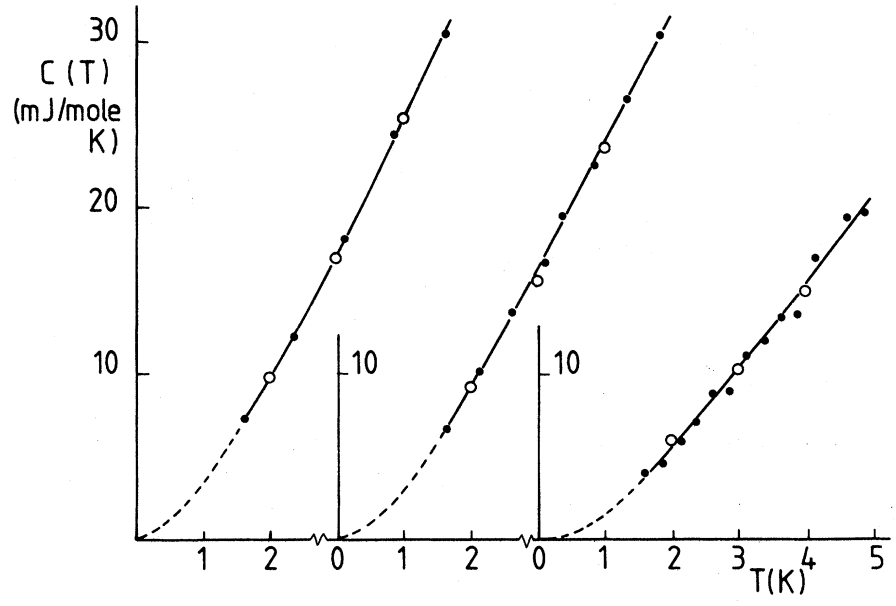


FIG. 5. Magnetic specific heat of *Cu*Mn alloys. (a) 2.5-at. % Mn, (b) 4.4-at. % Mn, (c) 9.7-at % Mn. ○ is estimated from Refs. 9–15. ● is estimated from $\Delta\rho(T)$ using Eq. (4). $\rho_\infty$ values in Table I.

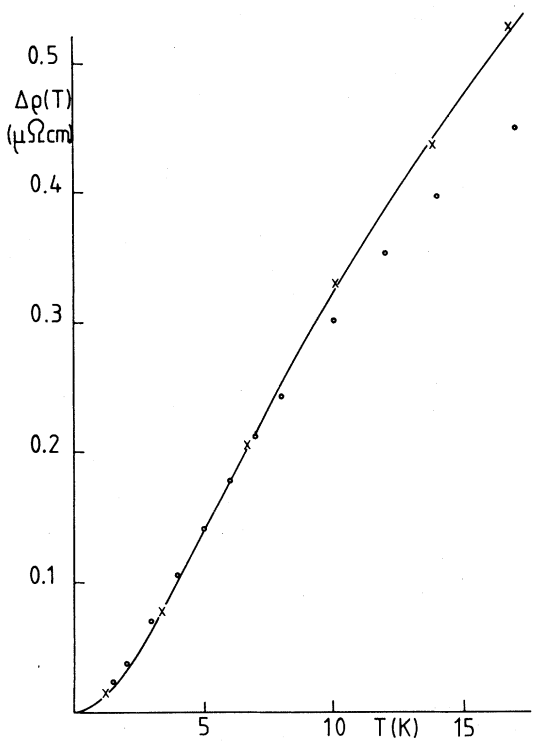


FIG. 6. $\Delta\rho(T)$ for 2.5-at. % *Cu*Mn. ○ denotes experiment and × is calculated with parameters given in Table I.

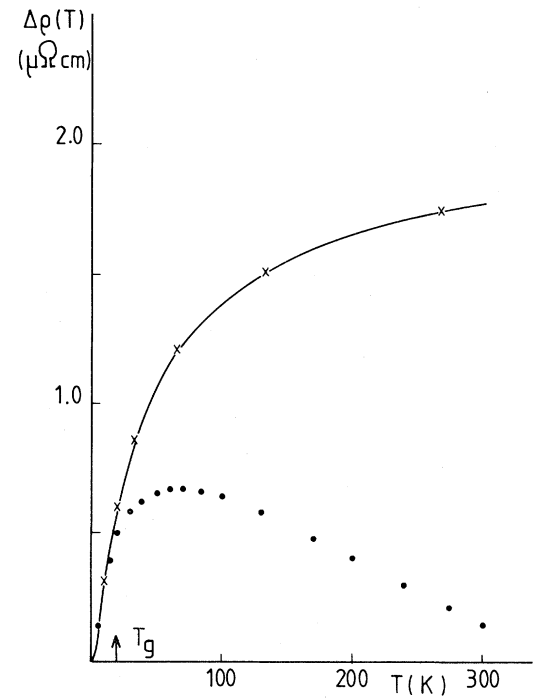


FIG. 7. $\Delta\rho(T)$ for 2.5-at. % *Cu*Mn. ○ denotes experiment and × is calculated with the same parameters as Fig. 6.

### *Ag*Mn

Again, we can carry out the same type of analysis using specific-heat data for a 1.1-at. % alloy[9] and $\Delta\rho(T)$ data at the same concentration. Results on 1.1-at. % *Ag*Mn are shown in Figs. 8 and 9. We should note that the specific heat is much higher than in *Cu*Mn, *Au*Fe, or *Au*Cr at similar concentrations, which is reflected in the analysis as a considerably lower $T^*$ for this alloy. As for *Cu*Mn there is a strong Kondo-resistivity term at high temperatures. We have also analyzed $\Delta\rho(T)$ data at 3.0-, 5.4-, and 9.7-at. % Mn.

### *Au*Cr

Here we have analyzed resistivity data for 0.9-, 1.5-, 3.3-, 4.9-, 7.9-, and 10.6-at. % Cr concentrations. A specific-heat measurement on a 0.9-at. % sample[16] can be used in conjunction with the 0.9-at. % resistivity data to estimate $\rho_\infty = 0.8\ \mu\Omega$ cm at this concentration. $T^*$ and $\rho_\infty$ values at other concentrations obtained from the log-log plot method are given in Table I. Some experimental and calculated $\Delta\rho(T)$ curves are shown in Figs. 10–12.

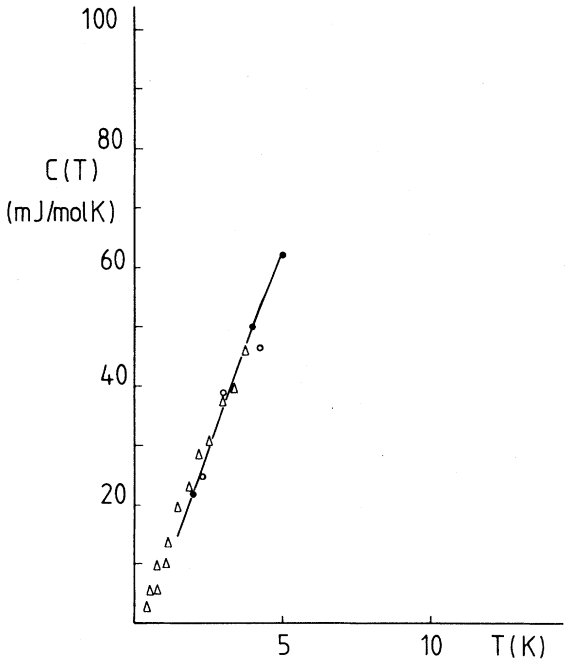


FIG. 8. Magnetic specific heat of 1.1-at. % *Ag*Mn. ● denotes direct measurement, Ref. 9. ○ is from $\Delta\rho(T)$ and Eq. (4). △ is from $\Delta\rho(T)$, Ref. 31, and Eq. (4). $\rho_\infty$ as given in Table I.

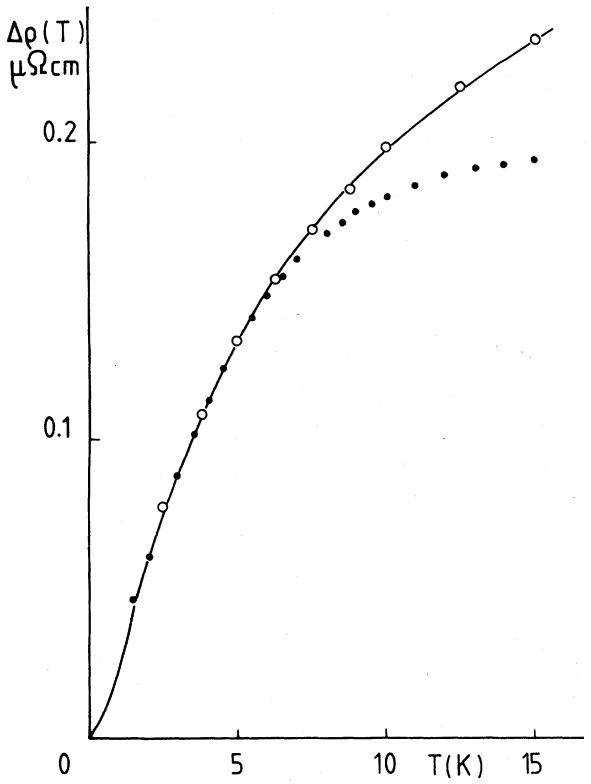


FIG. 9. $\Delta\rho(T)$ of 1.1-at.% *Ag*Mn. ● denotes experiment and ○ is calculated with parameters of Table I.

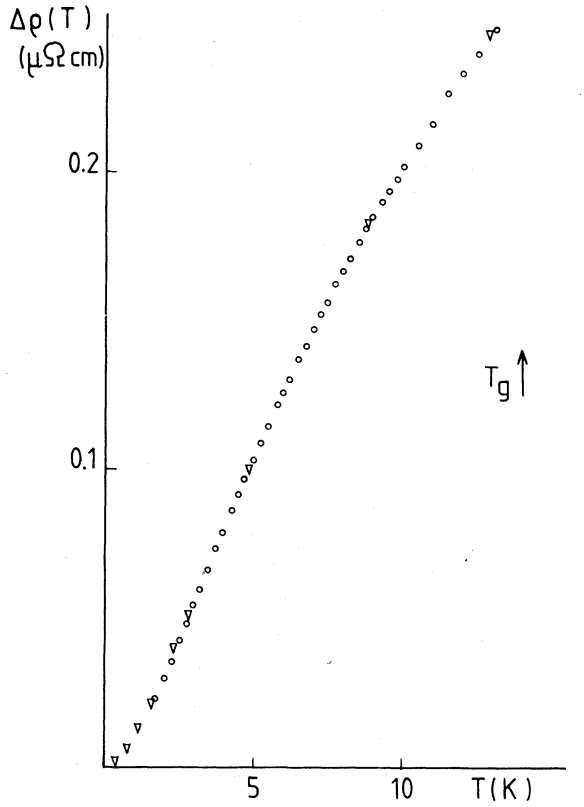


FIG. 10. $\Delta\rho(T)$ of 0.9-at.% *Au*Cr. ○ denotes experiment and ▽ is calculated with parameters of Table I.

Again we can compare high-temperature behavior where the Kondo effect is strong with data on dilute alloys from Teixiera[21]; as for *Cu*Mn the tie-up is satisfactory.

### *Au*Mn

For these alloys we have only resistivity data to go on, as we have found no specific-heat results in the appropriate concentration range. Resistivity results have been analyzed for 1.5-, 2.8-, 4.6-, 7.7-, and 11.8-at.% Mn. For the two most concentrated alloys the $\Delta\rho(T)$ curves deviated significantly from the $f(T/T^*)$ form, which had given a satisfactory fit for the other alloys.

## DISCUSSION

### Form of $\Delta\rho(T)$ curves

The analysis of the results on this wide range of spin-glasses has shown that up to $T_g$, $\Delta\rho(T)$ in each case is nearly of the form

$$\Delta\rho(T)=\rho_\infty f(T/T^*)\,,$$

where $f$ is the function we have calculated using the Walker-Walstedt density-of-states histogram. In fact the experimental curves for different alloys are not identical (*Au*Fe and *Au*Cr giving the best agreement with the model) but further work will be needed to establish if these differences have a physical significance and if there are definite trends in the data. Allowing for the Kondo effect, the $\rho_\infty$ values estimated from the low-temperature analysis seem compatible with the observed high-temperature behavior. The fact that in this type of alloy strong correlations remain well above $T_g$ has been recognized for a long time; at $T\simeq T_g$, $\Delta\rho(T)$ is only about 30% of the free-spin saturation value $\rho_\infty$, because spin flips are still considerably hindered by interactions.

It appears that the model we have used is satisfactory and that the Walker-Walstedt excitation density of states is reasonably close to reality in these alloys. Detailed differences may well show up in a more complete analysis but there seems little doubt as to the existence of these excitations.

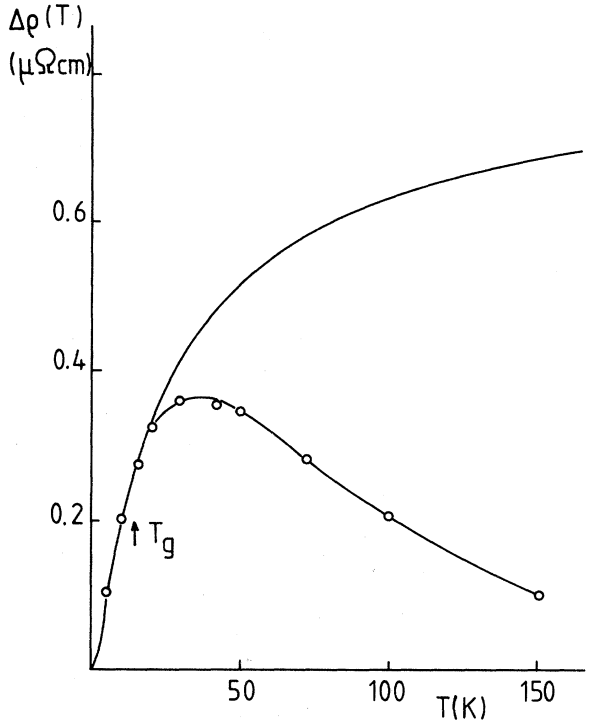


FIG. 11. $\Delta\rho(T)$ of 0.9-at. % *Au*Cr. o is experimental and — is calculated with the same parameters as Fig. 10.

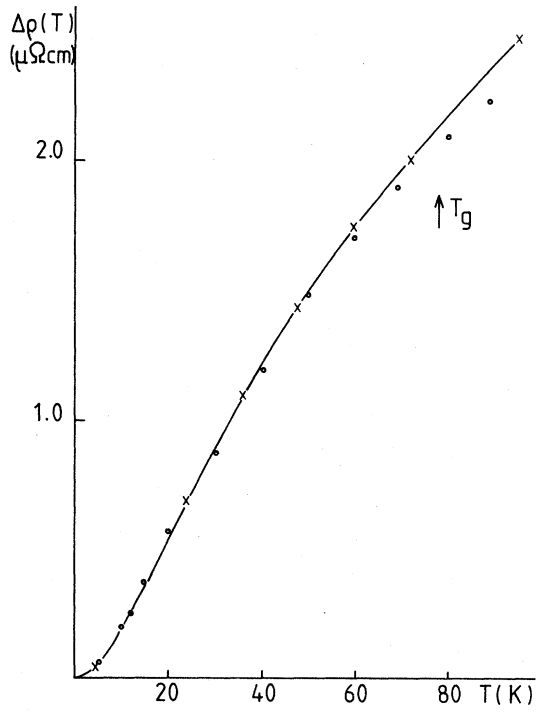


FIG. 12. $\Delta\rho(T)$ for 7.9-at. % *Au*Cr. o denotes experiment and × is calculated, parameters given in Table I.

In the past there has been some argument as to the limiting form of the low-temperature resistivity of spin-glasses—a $T^{3/2}$ behavior having been observed in a large number of cases. We have plotted, in Fig. 13, the calculated $\Delta\rho(T)$ against $T^{3/2}$. It can be seen that on this model the $T^{3/2}$ law can be expected to hold rather well over a wide range of temperatures, approximately for $0.1 < T/T^* < 0.7$. In fact, it turns out that almost all experiments have actually been done in the temperature range $T > 0.1T^*$, which would explain why the apparent $T^{3/2}$ limiting behavior has been observed in most cases. Exceptions are 7.9- and 10.6-at. % *Au*Cr (Ref. 5) where $T^*$ is very high, and in alloys where measurements were done to below 0.3 K.[23] In these cases, a $T^2$ dependence was observed, which appears to confirm the model prediction that $\Delta\rho(T)$ varies faster than $T^{3/2}$ for $T < 0.1T^*$. To obtain the true low-temperature limiting behavior, which would be interesting so we could check on the initial excitation density of states $P(\Delta)$ as $\Delta \to 0$, we would require measurements on high-$T^*$ samples at $T$ well below 1 K. If the arguments given by Walstedt[17] are correct, $\Delta\rho(T)$ should behave as $T^3$ when $T \to 0$.

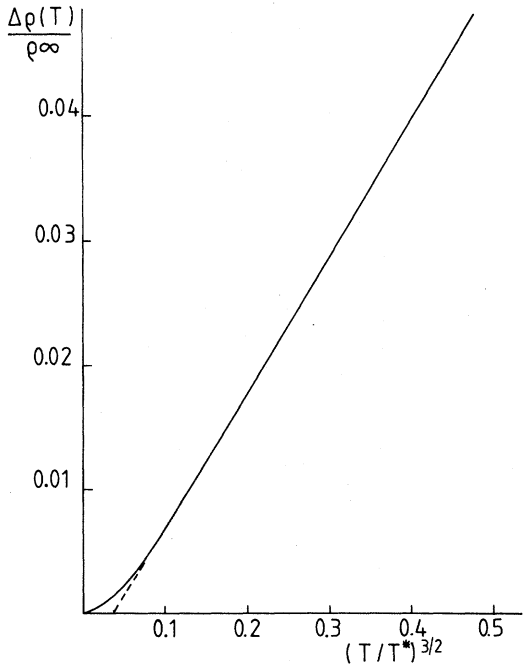


FIG. 13. Calculated $\Delta\rho(T)/\rho_\infty$ as a function of $(T/T^*)^{3/2}$.

### Variation of $\rho_\infty$, $T^*$

These are the two parameters that are sufficient to describe the resistivity behavior below $T_g$. As can be seen in Figs. 14 and 15, both $\rho_\infty$ and $T^*$ vary regularly with concentration in each alloy series, increasing more or less proportionally to concentration. $\rho_\infty$ expresses the local spin conduction-electron interaction strength, and we will postpone its discussion to the next section.

$T^*$ is a parameter that expresses the energy scale of the excitation spectrum. As the impurity concentration increases the interactions will become stronger so $T^*$ will increase; this is what is observed. What is more interesting is that $T^*$ and the spin-glass freezing temperature appear to scale the same way; for all concentrations and for all series of alloys we find $T_g \simeq (3.0 \pm 0.5) T^*$. Despite the intrinsic uncertainty in the estimate of $T^*$, this is a strong indication that the interactions which determine the excitation spectrum also determine $T_g$. If we consider the excitations as bosons and calculate the total number of excitations, we find at $T = 3.0 T^*$ the number of excitations per impurity is rather close to 0.5. We can conjecture that as in ferromagnets, magnetic order breaks down when the number of excitations per magnetic site exceeds a certain value. It has been suggested that non-RKKY couplings fix the value of $T_g$ (Ref. 24); this would not be in agreement with the present conclusion.

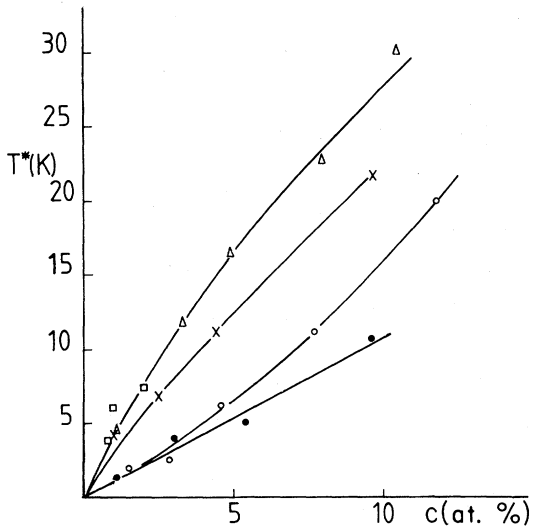


FIG. 14. Fitting parameter $T^*$ as a function of concentration $c$. △, *Au*Cr; □, *Au*Fe; ×, *Cu*Mn; ○, *Au*Mn; ●, *Ag*Mn.

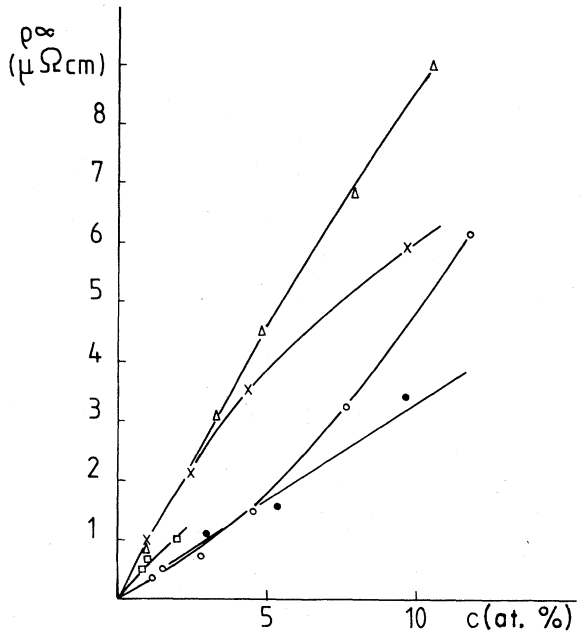


FIG. 15. Fitting parameter $\rho_\infty$ as a function of concentration $c$. △, *Au*Cr; □, *Au*Fe; ×, *Cu*Mn; ○, *Au*Mn; ●, *Ag*Mn.

### Relaxation

A number of different techniques have been used to estimate the local spin-relaxation time in dilute alloys—NMR, EPR, neutron scattering, and muon spin rotation ($\mu$SR).[25–29] We can also use the resistivity data. At high temperatures, for isolated noninteracting local moments, the spin-flip scattering process involves the scattering of a conduction electron and the simultaneous reorientation of the local moment. The spin-flip scattering resistivity gives a measure of the number of such events per second and hence can be interpreted in terms of the local-moment relaxation rate. If the Korringa local-moment spin-lattice relaxation time is $\tau_1$ (defined in just the same way as the nuclear $T_1$), for a free-electron host conduction band we can derive

$$\tau_1 = \frac{4}{9Z} \left[ \frac{T_F}{T} \right] S(S+1) c \tau_\rho^m , \tag{5}$$

where $Z$ is the number of conduction electrons per atom in the host, $T_F$ is the Fermi temperature, $c$ is the impurity concentration, and $\tau_\rho^m$ is a magnetic transport property relaxation time related to $\rho_\infty$ in the usual way by $\tau_\rho^m = ne^2/m\rho_\infty$, where $n$ is the number of electrons per unit volume and $m$ the electron mass.

Taking $\rho_\infty$ values as estimated experimentally

above, (Table I) we derive values for $\tau_1$ at 300 K for dilute alloys of the various systems as shown in Table II. These values can be compared with estimates of the Korringa relaxation rates by other techniques. In *Cu*Mn the absolute value is in quite reasonable agreement with[25] NMR and neutron[27] data considering that our assumption of a free-electron conduction band is a first approximation so that a correction factor should appear in Eq. (5). The relative values of the relaxation rates in the different systems are also satisfactory—in agreement with the neutron data,[27] the resistivity results indicate that in *Au*Mn and *Ag*Mn the relaxation rate is about 2–3 times slower than in *Cu*Mn at the same temperature. This lends credibility to the resistivity values for the relaxation rates in *Au*Fe and *Au*Cr where no neutron results exist and where the NMR technique would be very difficult to apply. We can note that $\rho_\infty$ and $T^*$ are high in the same alloys—this is to be expected as both will increase when the local coupling $J_{sd}$ increases.

At low temperatures where interactions are important the problem of the interpretation of a local-moment relaxation time is much more complex. We can still use Eq. (5) to estimate a relaxation rate which is the excitation conduction-electron scattering rate normalized to the number of spins. We can compare the relaxation time $\tau_1^*$ to the $\mu$SR estimate of the local spin-correlation time $\tau_c$ (Fig. 16). We have reproduced the $\tau_c$ values of Ref. 28 even though later longitudinal polarization measurements[30] showed that these $\tau_c$ values were meaningful for $T > T_g$, while for $T < T_g$ a single relaxation-time approach is too simplified. In this range, static components of local moments dominate the $\mu$SR behavior, but there remain some relaxation processes with $\tau_c \sim 10^{-5}$ sec at $T \sim 0.5 T_g$.[30]

TABLE II. Local-moment relaxation time at 300 K estimated using $\rho_\infty$ and Eq. (5). Values estimated from NMR (Ref. 25) and neutron scattering (Ref. 27) are given for comparison.

| Alloy | $\rho_\infty/c$ ($\mu\Omega$ cm/at. %) | $10^{13}\tau_1$ (sec) at 300 K From Eq. (5) | From NMR, neutrons |
|---|---|---|---|
| *Cu*Mn | 1.0 | 2.5 | 2.8 (Ref. 27) 3.0 (Ref. 25) |
| *Ag*Mn | 0.35 | 7.1 | 5.5 (Ref. 27) |
| *Au*Mn | 0.3 | 8 | 8.3 (Ref. 27) |
| *Au*Fe | 0.6 | 4.2 | |
| *Au*Cr | 0.9 | 2.8 | |

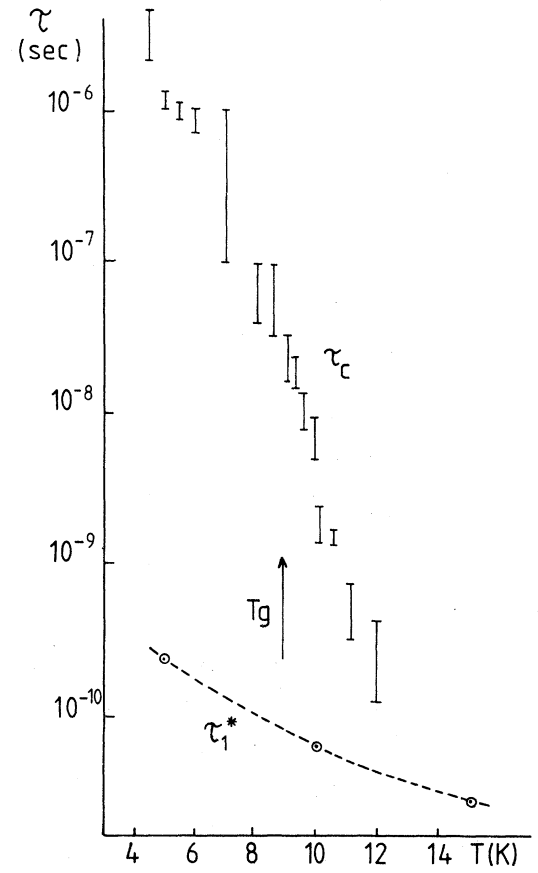


FIG. 16. Relaxation times $\tau_c$ (from $\mu$SR) and $\tau^*$ [from $\Delta\rho(T)$] for 1-at.% *Au*Fe. $\tau_c$ values from Ref. 28. See text.

In Fig. 16, it can be seen that $\tau_c$ and $\tau_1^*$ begin to diverge somewhere well above $T_g$; for $T \lesssim T_g$ inversion of a given spin occurs much more rarely than an excitation scattering time. At these temperatures, the excitation scatterings can be visualized in terms of rapid small-angle vibrations of any particular spin about its average direction to which a probe such as a muon is not sensitive.

We can give a qualitative picture for the relaxation behavior. We suggest that basically the relaxation of the interacting local moments by the conduction electrons is the fundamental process over the whole temperature range. Suppose we consider the low-energy states of the system as a large set of quasidegenerate ground states, each having a system of excited states built upon it. Call a ground state and its associated excited states a complex. Well above $T_g$ the total system can make transitions within and between all complexes, a situation equivalent to scattering by independent free spins. As $T_g$ is approached, certain intercomplex scatter-

ing rates become very slow; just below $T_g$ the system is frozen into a limited set of complexes and transitions into a whole class of other complexes will never occur (just as a macroscopic ferromagnet below $T_c$ will never spontaneously relax from magnetization ↑ to magnetization ↓). As $T$ is lowered further, the system will continue to shed attainable complexes and intercomplex transitions will slow down; well below $T_g$ over long periods the system is essentially frozen into one complex. In contrast to the ferromagnet, there will, however, remain infrequent transitions from one complex to another, by thermally activated multiexcitation barrier jumps. In going from one complex to another we can expect local spin directions to change orientation considerably.

Over the whole temperature range the excitation scattering rate only slows down very gradually; even at $T \simeq 0.5 T_g$, although the system is almost static, there are still frequent intracomplex transitions between the occupied ground state and its associated excited states. In a ferromagnet a hyperfine probe such as a muon "sees" only the time-averaged local field,[30] the equivalent here is the time average within a given complex, but there remains a low-frequency effect due to the rare intercomplex transition and its associated reorientations of local spins (see also discussion in Refs. 29, 30, and 32).

## CONCLUSION

We have analyzed the temperature-dependent part of the resistivity in a number of spin-glass alloys using the model of Ref. 3. We find the following.

(a) For each alloy system we obtain good agreement between resistivity and specific-heat data on the one hand and the expectations of the model using the Walker-Walstedt excitation description on the other.

(b) The spin-glass ordering temperature $T_g$ is approximately proportional to the excitation energy scaling parameter.

(c) We can derive a local spin-relaxation rate from the resistivity data which is consistent with estimates from other techniques. We can use the low-temperature resistivity data to help understand relaxation processes around and below $T_g$.

## ACKNOWLEDGMENT

We are very grateful to Professor J. A. Mydosh, who kindly put a large quantity of tabulated data at our disposal.

[1]M. T. Béal-Monod, Solid State Commun. 9, 1443 (1971); M. Rivier and K. Adkins, J. Phys. F 5, 1745 (1975); J. Seiden, C. R. Acad. Sci. 282B, 159 (1976); K. H. Fischer, Z. Phys. B 45, 53 (1979).
[2]L. R. Walker and R. E. Walstedt, Phys. Rev. Lett. 38, 514 (1977); L. R. Walker and R. E. Walstedt, Phys. Rev. B 22, 3816 (1980).
[3]I. A. Campbell, Phys. Rev. Lett. 47, 1473 (1981).
[4]J. A. Mydosh, P. J. Ford, M. P. Kawatra, and T. E. Whall, Phys. Rev. B 10, 2845 (1974).
[5]P. J. Ford and J. A. Mydosh, Phys. Rev. B 14, 2057 (1976).
[6]L. E. Wenger and P. H. Keesom, Phys. Rev. B 11, 3497 (1975).
[7]D. L. Martin, Phys. Rev. B 21, 1906 (1980).
[8]B. Dreyfus, J. Souletie, R. Tournier, and L. Weil, C. R. Acad. Sci. 259, 4266 (1964).
[9]F. J. du Chatenier and J. de Nobel, Physica 32, 1097 (1966).
[10]L. E. Wenger and P. H. Keesom, Phys. Rev. 13, 4053 (1976).
[11]D. L. Martin, Phys. Rev. B 21, 1906 (1980).
[12]D. L. Martin, Phys. Rev. B 20, 368 (1979).
[13]D. L. Martin, J. Phys. 39, C6-908 (1978).
[14]J. E. Zimmerman and F. E. Hoare, J. Phys. Chem. Soc. 17, 52 (1960).
[15]L. T. Crane and J. E. Zimmerman, J. Phys. Chem. Soc. 21, 310 (1961).
[16]T. Kemeny, G. J. Nieuwenhuys, and H. Algra, in *Proceedings of the 14th International Conference on Low Temperature Physics, LT14,* edited by M. Krusius and M. Vuorio (North-Holland, Amsterdam, 1975), p. 441.
[17]R. E. Walstedt, Phys. Rev. B 24, 1524 (1981).
[18]K. Matho and M. T. Béal-Monod, Phys. Rev. B 5, 1899 (1972).
[19]U. Larsen, Phys. Rev. B 18, 5014 (1978).
[20]K. H. Fischer (unpublished).
[21]J. Teixiera, thesis, Grenoble (unpublished).
[22]P. J. Ford, T. E. Whall, and J. W. Loram, Phys. Rev. B 2, 1547 (1970).
[23]O. Laborde and P. Radhakrishna, J. Phys. F 3, 1731 (1973).
[24]R. W. Walstedt and L. R. Walker, Phys. Rev. Lett. 47, 1624 (1981).
[25]H. Alloul, F. Hippert, and H. Ishii, J. Phys. F 9, 725 (1979).
[26]M. B. Salamon and R. M. Herman, Phys. Rev. Lett.

41, 1506 (1978).
[27]A. P. Murani, J. Magn. Magn. Mater. 25, 68 (1981).
[28]Y. J. Uemura, T. Yamazaki, R. S. Hayano, R. Nakai, and C. Y. Huang, Phys. Rev. Lett. 45, 583 (1980).
[29]D. E. Maclaughlin, Hyperfine Interact. 8, 749 (1981).
[30]Y. J. Uemura, K. Nishiyama, T. Yamazaki, and R. Nakai, Solid State Commun. 39, 461 (1981).
[31]D. Jha and M. H. Jericho, Phys. Rev. B 3, 147 (1971).
[32]A. J. Bray and M. A. Moore (unpublished).